Cell Death and Differentiation (2013) 20, 620–629

www.nature.com/cdd

Stabilization of p21 (Cip1/WAF1) following Tip60-dependent acetylation is required for p21-mediated DNA damage response

M-S Lee[1], J Seo[1], DY Choi[2], E-W Lee[1], A Ko[1], N-C Ha[3], J Bok Yoon[1], H-W Lee[1], K Pyo Kim[2] and J Song*[,1]

The molecular mechanisms controlling post-translational modifications of p21 have been pursued assiduously in recent years. Here, utilizing mass-spectrometry analysis and site-specific acetyl-p21 antibody, two lysine residues of p21, located at amino-acid sites 161 and 163, were identified as Tip60-mediated acetylation targets for the first time. Detection of adriamycin-induced p21 acetylation, which disappeared after Tip60 depletion with concomitant destabilization of p21 and disruption of G1 arrest, suggested that Tip60-mediated p21 acetylation is necessary for DNA damage-induced cell-cycle regulation. The ability of 2KQ, a mimetic of acetylated p21, to induce cell-cycle arrest and senescence was significantly enhanced in p21 null MEFs compared with those of cells expressing wild-type p21. Together, these observations demonstrate that Tip60-mediated p21 acetylation is a novel and essential regulatory process required for p21-dependent DNA damage-induced cell-cycle arrest.
Cell Death and Differentiation (2013) **20,** 620–629; doi:10.1038/cdd.2012.159; published online 14 December 2012

A plethora of cellular perturbations stimulate cells to halt their growth progression by activating numerous cell-cycle inhibitors and apoptotic factors. Among these, p21 is a key member whose major function is to suppress the activities of cyclin-dependent kinases (CDKs).[1,2] This, in turn, leads to cellular growth arrest at a certain stage of the cell cycle mainly as a result of the inhibition of RB or cyclin B phosphorylation.[2–4] The induction of p21 requires the presence of p53, a potent tumor suppressor, as its major transcriptional regulator.[5,6] In addition to transcriptional regulation, a variety of regulatory proteins that modulate the activity of p21 in its post-translational stage have been characterized.[7–13] For example, several E3 ligases, including CUL1, CUL4, and APC2 complexes, function to constitutively induce destabilization of p21 and facilitate cell-cycle progress.[9] In addition to these ligases, p21 levels are closely monitored under normal cellular conditions by other E3 ligases, such as MKRN1, p53RFP, and RNF126, in order to facilitate senescent-free progression.[11,13,14] The interaction of histone deacetylases (HDACs) with p21 was also identified in a recent study, suggesting a possible acetylation process for p21.[15]

Tip60, originally identified as HIV-1 interacting acetyltransferase, is a member of the MYST family, which contains MOZ, Ybf2/Sas2, and Sas2 motifs.[16,17] Tip60-mediated acetylation of H2AX, a member of the histone family of proteins that plays a major role in DNA repair, helps to enhance DNA dynamics upon DNA-damaging stresses.[18,19] On the other hand, non-histone proteins targeted by Tip60 include ATM, p53, and Myc, among others.[20,21] Tip60 can mediate the acetylation of p53 at the lysine residue 120, resulting in increased p53 transcriptional activity with the induction of PUMA and BAX.[22,23] Several studies have reported that the acetylase activity of Tip60 is enhanced by various stresses such as ER stress, serum deprivation, and DNA damage, including damage due to ionizing radiation and UV irradiation.[24–28] *In vivo* studies of Tip60 suggest that it is a haplo-insufficient tumor suppressor, the loss of which can lead to tumor formation in both humans and mice.[29] Taken together, the data presently available indicate that Tip60 is expected to have a significant role in tumorigenesis.

In these studies, we demonstrated that the role of Tip60 in mediating acetylation of p21 at its C-terminus is a novel and significant mechanism for post-translational regulation of cell-cycle progression.

Results

Inhibition of HDAC families promotes p21 acetylation and stabilization, which is reversed upon Tip60 depletion. Previous studies have shown that p21 transcription is regulated by the presence of HDAC inhibitors or Tip60.[30–32] Interestingly, while experiments using HepG2 and Hep3B cell lines confirmed these previous results, upon treatment with trichostatin A (TSA), an HDAC inhibitor, other cell lines such as HCT116 $p53^{+/+}$, A549, and HCT116 $p53^{-/-}$ exhibited dramatic p21 protein stability without any observed effect on p21 mRNA (Figure 1a; Supplementary Figures 1a and b). When the same cell lines were treated with TSA and

[1]Department of Biochemistry, College of Life Science and Biotechnology, Yonsei University, Seoul, Republic of Korea; [2]Department of Molecular Biotechnology, Institute of Biomedical Science and Technology, Konkuk University, Seoul, Republic of Korea and [3]Department of Manufacturing Pharmacy, College of Pharmacy, Pusan National University, Busan, Republic of Korea
*Corresponding author: J Song, Department of Biochemistry, Yonsei University, Yonsei-ro 50, Seodaemun-gu, Seoul 120-749, Republic of Korea.
Tel: +82 2 2123 5695; Fax: +82 2 362 9897; E-mail: jso678@yonsei.ac.kr
Keywords: p21 (Cip1/WAF1); Tip60; acetylation; cell-cycle arrest; DNA damage
Abbreviations: TSA, trichostatin A; SAHA, suberoylanilide hydroxamic acid; α-Acetyl K, anti-acetylated lysine antibodies; ADR, Adriamycin
Received 04.06.12; revised 06.11.12; accepted 07.11.12; Edited by A Villunger; published online 14.12.12

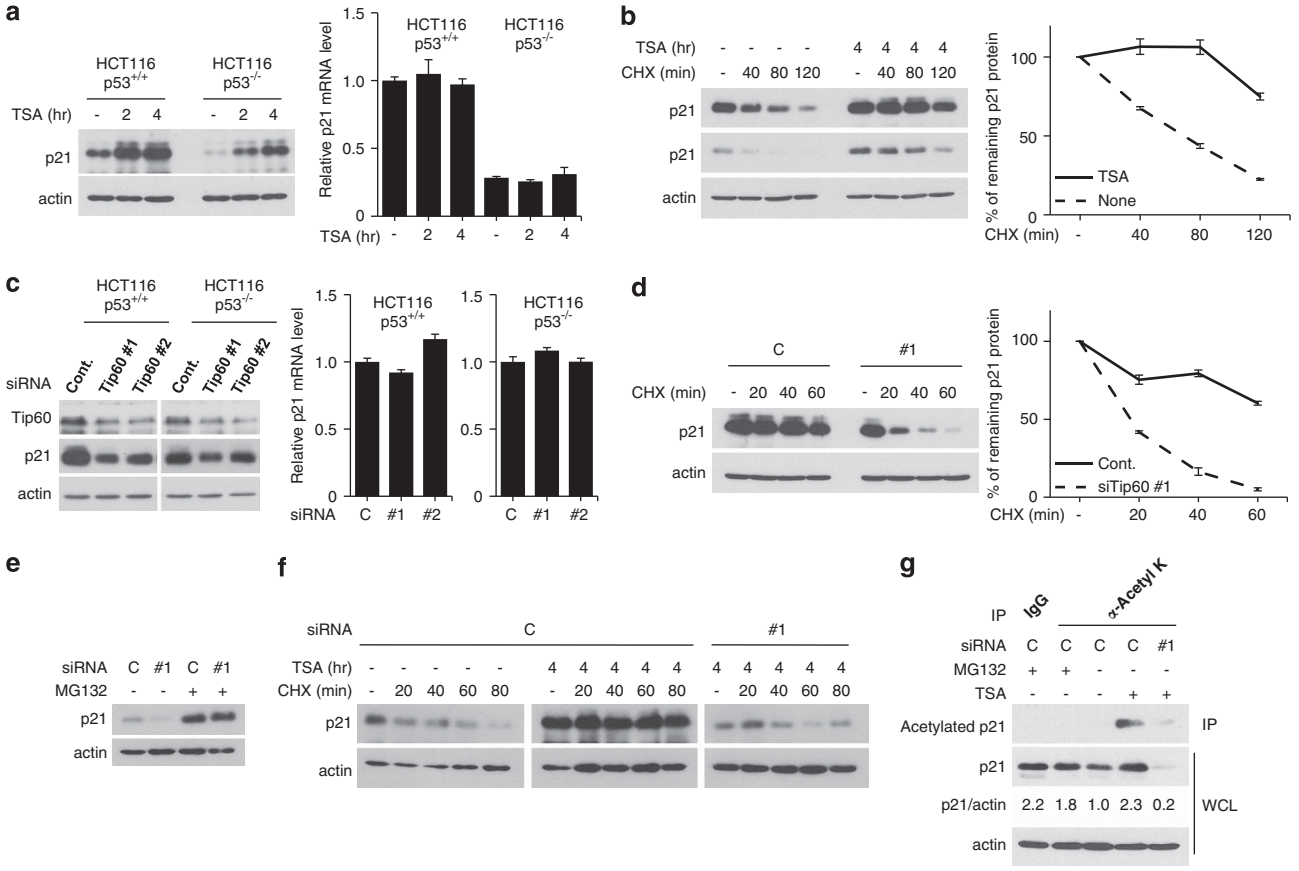

Figure 1 Trichostatin A (TSA), an HDAC family inhibitor, induces p21 acetylation and stabilization, the effect of which is diminished by Tip60 depletion. (**a**) TSA treatment increases p21 protein levels. HCT116 p53$^{+/+}$ and p53$^{-/-}$ cells were treated with 10 μM TSA, after which whole cell lysates (WCLs) were obtained and analyzed by immunoblotting (left panel). Concurrent with immunoblotting, the p21 mRNA expression was determined by qRT-PCR analysis (right panel). Relative p21 mRNA levels were normalized to GAPDH mRNA levels, and the presented values represent the fold change. Data are presented as the mean ± S.D. of three independent experiments. (**b**) TSA treatment increases the half-life of p21. HCT116 p53$^{+/+}$ cells were treated with TSA and CHX (100 μg/ml). Relative p21 proteins were calculated after normalizing to actin (right panel) (**c**) Depletion of Tip60 reduces p21 protein abundance without affecting mRNA levels. HCT116 p53$^{+/+}$ and p53$^{-/-}$ cells were transfected with control siRNA, Tip60 siRNA #1, or Tip60 siRNA #2 for 48 h. Proteins (left panel) and relative p21 mRNA levels (right panel) were analyzed as described above. (**d**, **e**) Tip60 depletion reduces the half-life of p21. Cells transfected with control siRNA or Tip60 siRNA#1 were treated with either CHX or MG132 (10 μM). Relative amounts of p21 were quantified and normalized to actin (right panel). (**f**) TSA-induced p21 stabilization is abrogated in the absence of Tip60. (**g**) TSA treatment induces p21 acetylation. Following transfection of HCT116 p53$^{+/+}$ cells with control siRNA or Tip60 siRNA#1, cells were treated with MG132 or TSA for 4 h. WCLs were immunoprecipitated using anti-acetylated lysine antibodies. C, #1, and #2 represent control siRNA, Tip60 siRNA #1, and Tip60 siRNA #2, respectively

cycloheximide (CHX), a translation inhibitor, there was an increase in the half-life of p21 in all cell lines tested (Figure1b; Supplementary Figure 2). Notably, U2OS was not significantly affected by TSA. SAHA and sodium butyrate, also HDAC inhibitors, displayed similar effects as TSA on HCT116 p53$^{+/+}$ cells in terms of stabilizing p21 (Supplementary Figure 3, data not shown). Overall, these data suggest that HDAC inhibition could be associated with p21 protein stabilization without affecting its mRNA in some cell lines.

The role of Tip60 in cell-cycle regulation is not well defined, which prompted us to evaluate its effects in association with the effects of TSA on p21. To this end, we first analyzed three Tip60 siRNAs, #1, #2, and #3, all of which were able to suppress the expression of endogenous Tip60 by 70–90% in the HCT116 p53$^{+/+}$ cell line (Supplementary Figure 4). Based on these observations, Tip60 siRNAs #1 or #2 were utilized for Tip60 ablation. Upon Tip60 ablation in the cell lines indicated above, decreases in endogenous p21 protein levels were detected (Figure 1c; Supplementary Figure 5a). While there were no significant changes in p21 mRNA upon Tip60 knockdown in HCT116 p53$^{+/+}$, U2OS, A549 or HCT116 p53$^{-/-}$ cells, HepG2 and Hep3B cells showed a reduction in p21 mRNA levels (Figure 1c; Supplementary Figure 5b). Treatment with CHX also resulted in a substantial reduction in the half-life of p21 when Tip60 was ablated (Figure 1d; Supplementary Figure 6). The reduced levels of p21 under Tip60 knockdown in HCT116 p53$^{+/+}$ cells were completely recovered upon treatment with MG132, a proteasome inhibitor, suggesting that the p21 protein levels are regulated at the post-translational level in this case (Figure 1e). Lastly, the stabilizing effects of TSA on p21 were almost completely abolished upon Tip60 knockdown (Figure 1f).

We observed increased acetylated p21 levels upon TSA treatment as detected by anti-acetylated lysine (α-Acetyl K) antibodies. This p21 acetylation process was not detected

upon depletion of Tip60 due to the destabilization of p21 (Figure 1g, lanes 4 and 5). Unlike the stabilization of p21 by TSA, p21 stabilized by MG132, a proteasome inhibitor, was not acetylated, as shown in lane 2 of Figure 1g. In conclusion, Tip60 seems to be necessary for maintaining the stability of p21 protein, since Tip60 ablation induces a drastic destabilization of p21, regardless of TSA treatment, without affecting p21 mRNA levels.

The HAT motif-containing domain of Tip60 is required for interaction with the C-terminus of p21. The correlation between the levels of Tip60 and p21 proteins next led us to examine if the proteins could interact with each other. Immunoprecipitation analyses showed that exogenously expressed or endogenous proteins could indeed interact with each other (Supplementary Figures 7a–c). Using recombinant proteins (His-p21 and GST-Tip60) in GST-pulldown assays, we confirmed that the two proteins were able to directly bind (Supplementary Figure 7d). Domain mapping showed that the C-terminus of p21, a region consisting of residues 139 and 164 of p21, was responsible for its interaction with Tip60 (Supplementary Figure 7e). Immunofluorescent analyses showed that Tip60 and p21 or its truncated forms were mostly colocalized, excluding the possible effects of cellular localization on complex formation between Tip60 and p21 mutants (Supplementary Figure 8).

Multiple C-terminal domains of Tip60 might also be responsible for its interaction with p21 (Supplementary Figure 9a). Specifically, Tip60 fragments 212–364 and 390–511, both of which lack the histone acetyltransferase (HAT) motif, displayed a rather weak binding affinity for p21 compared with that of the 365–511 fragment containing the HAT motif. These observations were further confirmed using a HAT deletion Tip60 mutant (ΔHAT), HAT mut[33] or Tip60 wild-type (WT). The results demonstrated a very weak interaction between p21 and ΔHAT but not with others, suggesting that the HAT domain is necessary for p21 interaction (Supplementary Figure 9b). In conclusion, the data related to binding between Tip60 and p21 suggest that the C-terminus of each protein is required for their interaction.

Tip60 stabilizes p21 at the post-translational stage. The destabilization of p21 in the absence of Tip60 and the direct interaction between the two proteins prompted us to ask if there was a possible role for Tip60 in mediating p21 protein stabilization. Increasing concentrations of overexpressed Tip60 led to corresponding stabilization of exogenous and endogenous p21 (Figures 2a and b). The assumingly saturated concentrations of p21 protein following treatment with MG132 were also achieved by overexpressing Tip60, implying that Tip60 itself might help stabilize p21 protein by suppressing proteasome-dependent degradation of p21 (Figure 2c). The half-life of exogenous p21 as determined

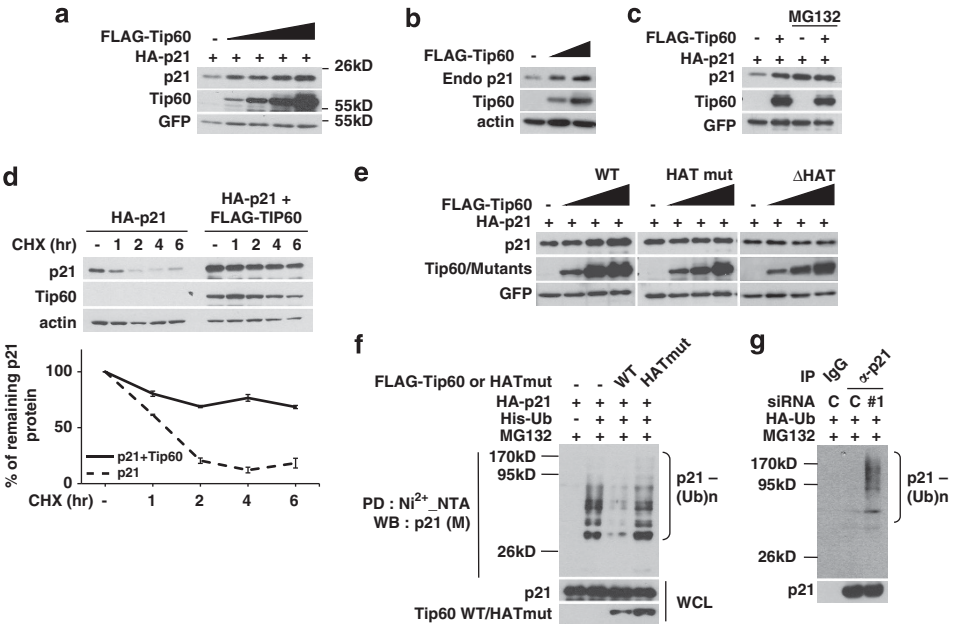

Figure 2 Tip60 induces post-translational stabilization of p21. (**a**) Exogenous Tip60 upregulates exogenous p21 protein levels. Combinations of plasmids expressing FLAG-Tip60, HA-p21, and GFP were transfected into H1299 cells. WCLs were analyzed by immunoblotting. GFP was used as a control. (**b**) Exogenous Tip60 upregulates endogenous p21 protein levels. Extracts of H1299 cells transfected with plasmids expressing Tip60 were analyzed by immunoblotting. (**c**) Tip60 stabilized p21 protein to a similar level as observed with MG132 treatment. Following transfection of H1299 cells with combinations of plasmids as indicated, cells were treated with or without 10 μM MG132 for 6 h (**d**) The presence of Tip60 prolonged the half-life of p21. H1299 cells were transfected with plasmids as indicated. CHX was then added to the cells before harvest. (**e**) p21 is stabilized by WT Tip60 but not acetyltransferase defective mutants. Combinations of plasmids were transfected as indicated in H1299 cells. (**f**) Tip60 but not HAT mut abolishes the poly-ubiquitination of p21. Combinations of plasmids were transfected as indicated into H1299 cells with MG132 for 6 h before harvest. The ubiquitination assay under denaturation condition was conducted. Ubiquitinated forms of p21 were detected using anti-p21 antibodies (upper panel). (**g**) Tip60 depletion induces the ubiquitination of p21. Control siRNA or Tip60 #1 siRNA were transfected in HCT116 p53$^{+/+}$ cells and then transiently transfected with the constructs expressing HA-Ub. WCLs were analyzed using the ubiquitination assay under denaturation condition. Ubiquitinated forms of p21 were detected using anti-HA antibodies (upper panel) and immunoprecipitated p21 were detected in bottom panel

by CHX treatment was about 1 h in our hands, while p21 was minimally degraded in the presence of Tip60 during the course of 6 h, further confirming the post-translational stabilizing effects of Tip60 on p21 (Figure 2d). Since Tip60 is an acetyltransferase containing a HAT domain, we assumed that the acetylation activity of Tip60 was an essential factor for p21 stabilization. To address this possibility, two Tip60 mutants, HAT mut and ΔHAT, along with Tip60 WT were evaluated for the ability to stabilize p21. The Tip60-mediated stabilization analyses showed that, unlike Tip60 WT, both mutants were unable to stabilize p21 (Figure 2e). The failure of HAT mut to stabilize p21 suggests that its acetyltransferase activity might be essential for p21 stabilization. One possible explanation for the stabilization of p21 in the presence of Tip60 is that Tip60 might disrupt ubiquitination of p21. Consistent with this possibility, the addition of Tip60 but not of HAT mut was able to suppress exogenous p21 ubiquitination under denaturing conditions (Figure 2f). Tip60 ablation increased levels of endogenously ubiquitinated p21 under denaturing conditions, indicating that Tip60 might negatively regulate p21 ubiquitination and degradation processes (Figure 2g). In both cases, general ubiquitination analyses were performed without any specific E3 ligases, as previously reported.[13,34] In summary, the intact acetyltransferase activity of Tip60 was required for p21 stabilization, which likely occurred through the direct suppression of p21 ubiquitination. These observations suggest that acetylation of p21 by Tip60 might hinder p21 ubiquitination and its subsequent degradation.

The K161 and K163 sites of p21 are major targets for Tip60-mediated acetylation. The results of our study thus far suggested that Tip60 directly mediates p21 stabilization through the possible acetylation of p21. To confirm this possibility, HA-p21 was immunoprecipitated in the presence or absence of Tip60 using α-Acetyl K antibodies. The data indicated that exogenous HA-p21 was immunoprecipitated by these antibodies only in the presence of WT Tip60 (Figure 3a). Specifically, and consistent with our stabilization data, co-expression of the HAT mut with p21 did not lead to the immunoprecipitation of p21 by α-Acetyl K antibodies (Figure 3b). These data implied the possibility that the process of p21 acetylation might be linked with p21 stabilization. Since the above results indicated that p21 could be acetylated, we next carried out immunoprecipitation/mass spectrometry (IP-mass spec) analyses. IP-mass spec was performed using immunoprecipitated FLAG-p21 in the presence of exogenous Tip60 and revealed two potential acetylation sites, namely, lysine residues positioned at sites 161 and 163 in the C-terminus of p21 (Figure 3c). Conversely, IP-mass spec of immunoprecipitated FLAG-p21 in the absence of Tip60 displayed no such results, as shown in Supplementary Figure 10.

The two lysine sites identified by IP-mass spec are conserved across various mammalian species including human and mouse (Figure 4a). Based on these observations, we constructed three point mutants of p21, K161R, K163R, and 2KR (K161R, K163R), which have arginines substituted for either one or both lysines at sites 161 and 163. There was no significant difference in the binding affinity of the mutants toward Tip60 (Figure 4b); however, none of the mutants was acetylated in the presence of Tip60 (Figure 4c). As both lysine sites appeared to be necessary for the acetylation process, we decided to employ 2KR for further *in vitro* acetylation

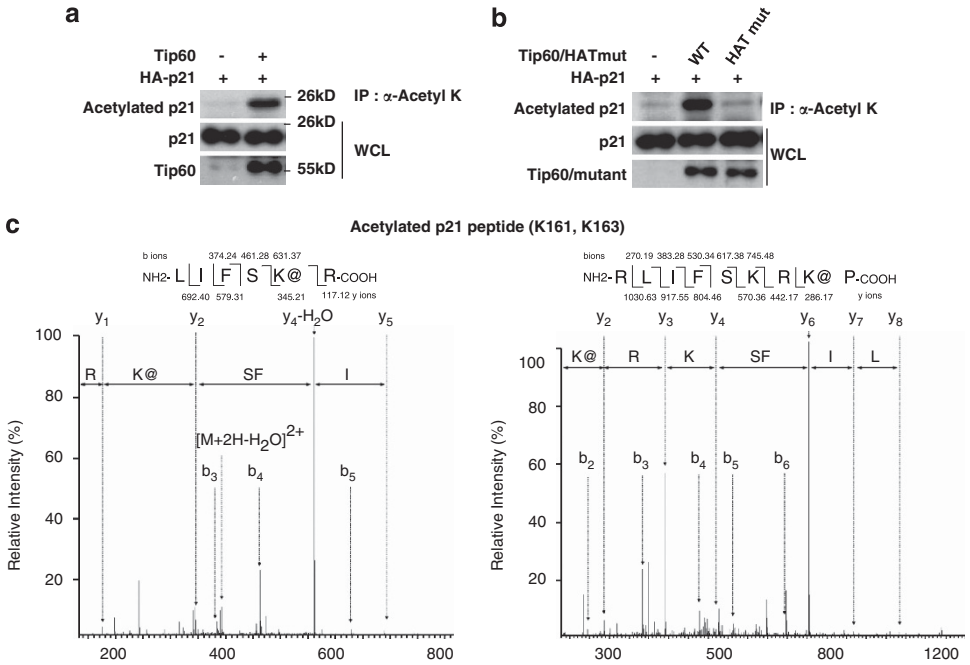

Figure 3 Identification of K161 and K163 sites within human p21 targeted by Tip60-mediated acetylation. (**a**, **b**) Tip60 acetylates p21. Plasmids expressing HA-p21 were expressed in the presence or absence of plasmids expressing Tip60 or HAT mut. The resulting WCLs were immunoprecipitated using α-Acetyl K followed by immunoblotting with anti-p21 and anti-Tip60 antibodies. (**c**) Mass-spectrometry analysis of the peptides containing K161, 163 of p21 (as indicated in Supplementary Figure 3) or acetylated K161, K163 of p21. Preparation of peptides and mass-spectrometry analysis protocol are described in Materials and Methods

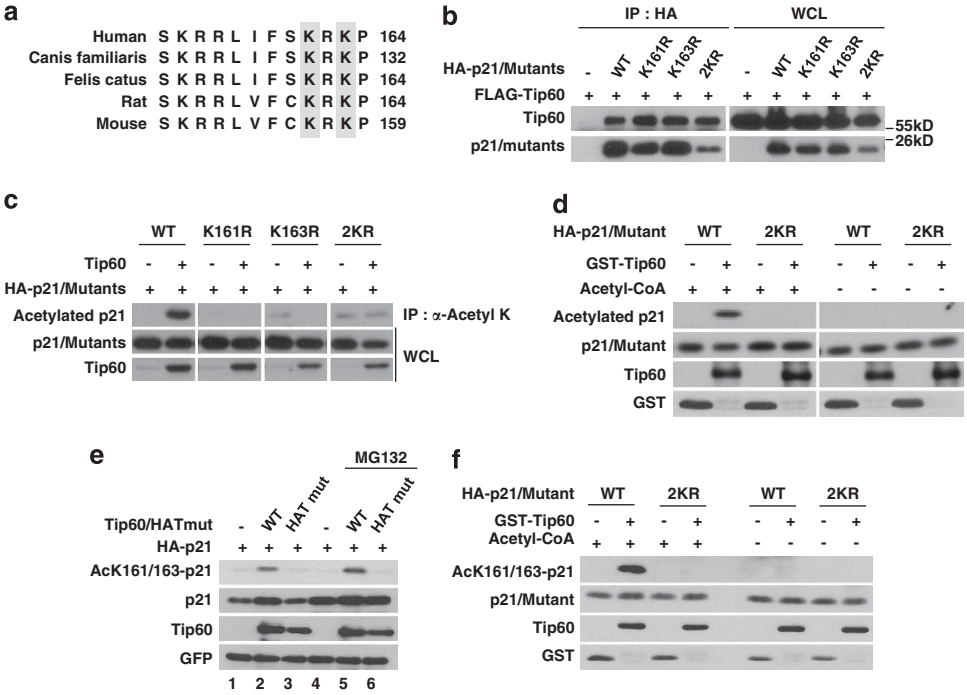

Figure 4 Tip60 specifically and directly acetylates K161 and K163 sites. (**a**) Alignment of the C-terminal domain of p21, including K161 and K163, from human and other species; conserved lysine sites are grey shaded. (**b**) Interaction of Tip60 and p21 or its lysine mutants. Combinations of plasmids were transfected as indicated into 293T cells. WCLs were immunoprecipitated with anti-HA antibodies. (**c**) Both p21 lysine sites 161 and 163 are required for efficient Tip60-mediated acetylation. Plasmids expressing HA-p21 or mutants were transfected into H1299 cells with or without a Tip60-expressing plasmid. Acetylated p21 was identified using α-Acetyl K antibodies as described in Figure 3a. (**d**) *In vitro* acetylation of p21 demonstrates that Tip60 directly acetylates p21 at sites 161 and 163. *In vitro* transcribed and translated p21 or 2KR were incubated with recombinant GST-Tip60 and acetyl-CoA as indicated. The samples were immunoblotted using α-Acetyl K, anti-HA, or anti-GST antibodies. (**e**) p21 is acetylated only in the presence of Tip60 but not in the presence of HAT mut or MG132. Following transfection of H1299 cells with the indicated combinations of plasmids expressing Tip60, HAT mut, HA-p21, or GFP, cells were treated with or without MG132. After immunoblotting of WCLs, acetylated p21 was detected using α-AcK161/163-p21, and total p21 levels were detected using anti-HA antibodies. (**f**) *In vitro* acetylation of p21 detected by α-AcK161/163-p21 antibodies demonstrating Tip60-mediated acetylation of p21 at sites 161 and 163. *In vitro* acetylation assays were performed as described in (**d**). Acetylated p21 was identified using α-AcK161/163-p21 antibodies

analyses. Accordingly, p21 WT and 2KR were expressed using the reticulocyte lysate system followed by the addition of recombinant GST-Tip60 with or without acetyl-CoA. The data showed that only p21 WT but not 2KR was acetylated under these conditions, further confirming that sites 161 and 163 of p21 are targeted by Tip60 for acetylation (Figure 4d).

To more accurately study p21 acetylation, we developed antibodies (α-AcK161/163-p21) that specifically identify the acetylated form of p21 at sites 161 and 163 by employing acetylated p21 C-terminal peptides as antigens. These antibodies are able to detect only acetylated p21 in the presence of Tip60 (Figure 4e, lanes 1–3). Since there was a substantial increase in p21 levels with Tip60 WT co-expression compared with those in the control or HAT mut, acetylated p21 levels were further detected with concomitant MG132 treatment. The results showed that, even with the increased levels of p21 in the presence of MG132, p21 co-expressed with Tip60 exhibited acetylated forms, while others did not (Figure 4e, lanes 4–6). Finally, using an *in vitro* acetylation analysis as shown in Figure 4f, we were able to detect the acetylated form of p21 in WT p21 but not in 2KR using α-AcK161/163-p21 antibodies, further confirming the acetylation of p21 at sites 161 and 163 (Figure 4f). In conclusion, we were able to detect p21 acetylation sites at 161 and 163 lysine residues employing IP-mass analyses. Using anti-acetylated p21 as well as anti-acetylated lysine antibodies, the p21 acetylated forms were detected in the presence of Tip60, thereby validating the IP-mass spec findings.

p21 acetylation at sites 161 and 163 is required for stabilization of functional p21 after DNA-damaging stress. We next investigated the physiological importance of p21 acetylation at lysine sites 161 and 163. Treatment of HCT116 $p53^{+/+}$ cells with sublethal amount of ADR increased p21 protein abundance with simultaneous increase of p21 mRNA (Figure 5a). Under Tip60 ablation, on the other hand, the protein levels of p21 were drastically decreased without much effect on mRNA levels (Figure 5a). There was no change in the protein levels of p53 with or without Tip60. Similar observations were obtained using HCT116 and U2OS cells, with different DNA-damaging agents such as etoposide (Supplementary Figure 11). In accordance with these data, the half-life of p21 was also decreased in ADR-treated cells under Tip60 depletion (Figure 5b). Next, the status of p21 acetylation under various different conditions was tested. The results showed that acetylated p21 detected using α-AcK161/163-p21 antibodies were only observed with ADR treatment but not with MG132 (Figure 5c). Conversely, the stabilization of p21 was completely abolished by the absence of Tip60, possibly due to the lack of acetylated p21 (Figure 5d). One possible

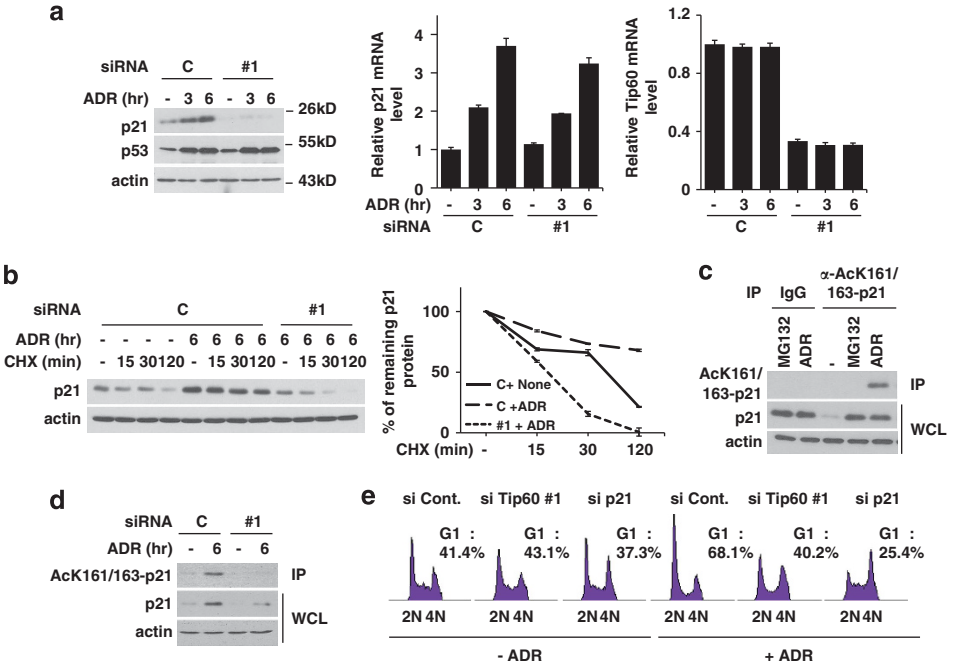

Figure 5 Tip60-mediated acetylation of p21 is required for DNA damage-induced cell-cycle arrest. (**a**) ADR-induced p21 is destabilized following depletion of Tip60. HCT116 p53$^{+/+}$ cells were treated with 1 μM ADR. WCLs were analyzed by immunoblotting using anti-p21 and anti-actin antibodies (left panel). Concurrently, mRNA levels of p21 and Tip60 were analyzed by qRT-PCR analysis (right panel) as shown in Figure 1a. (**b**) Tip60 ablation prolonged p21 protein half-life. HCT116 p53$^{+/+}$ cells transfected with control siRNA or Tip60 #1 siRNA were treated with or without 1 μM ADR for 6 h in the absence or presence of CHX (100 μg/ml): WCLs were analyzed as described above (left panel). Representative results of three independent experiments are shown. Relative p21 proteins were calculated after normalizing to actin (right panel). (**c**) ADR treatment induces p21 acetylation. WCLs from HCT116 p53$^{+/+}$ cells treated with MG132 (10 μM) or ADR (1 μM) were immunoprecipitated using α-AcK161/163-p21 antibodies followed by detection with an anti-p21 antibody (upper panel). Total expression of p21 is shown in the bottom panel along with actin controls. (**d**) Tip60 depletion abrogates ADR-induced p21 acetylation. HCT116 p53$^{+/+}$ cells transfected with control siRNA or Tip60 #1 siRNA were treated with 1 μM ADR before harvest, after which the abundance of acetylated p21 was identified as described in (**d**). (**e**) Tip60 ablation disrupts ADR-induced G1 cell-cycle arrest. RNAi-mediated Tip60-depleted HCT116 p53$^{+/+}$ cells were treated with ADR for 24 h before harvest. The cells were stained with propidium iodide and cell-cycle populations were determined by fluorescence-activated cell sorting analysis

explanation for the increase of p21 acetylation by Tip60 under ADR-induced DNA damage is that the levels of p21 binding to Tip60 were increased upon DNA damage (Supplementary Figure 12a). Consistent with these observations, the binding between Tip60 and its substrate p53 is increased upon DNA-damaging stress as reported previously.[22] Since p21 levels were decreased upon treatment of cells with a lethal amount of ADR, we further tested whether p21 could still interact with Tip60 under these conditions. The results showed that under lethal conditions, binding of p21 to Tip60 was significantly reduced, while binding of p53 to Tip60 was unchanged (Supplementary Figure 12b). These results were consistent with observations that the amount of acetylated p21 drastically decreased under lethal conditions (Supplementary Figure 13). It is not currently known how these processes occur under various DNA-damaging conditions.

Finally, as expected, Tip60 ablation eradicated ADR-induced cell-cycle arrest, which is prompted by the induction of p21 (Figure 5e). Here, either Tip60 or p21 ablation prevented cells from going through G1 arrest. Likewise, Tip60 depletion fully induces the decrease in p21 protein levels under DNA damage and disrupts the damage-induced cell-cycle arrest in IMR90 primary human fibroblasts (Supplementary Figure 14). Overall, these data suggest that the presence of Tip60 and its ability to acetylate p21 are necessary post-translational modifications for DNA damage-induced cell-cycle arrest. Under lethal conditions, however, the process of acetylation of p21 by Tip60 was blocked. In conclusion, stabilization of p21 upon its induction by DNA-damaging agents requires p21 acetylation activity of Tip60.

The acetylation of p21 counteracts the ubiquitination process of p21. We next generated an acetylated p21 mimetic, named 2KQ, by replacing the lysine residues at positions 161 and 163 with glutamine. First, when CHX was employed to measure the half-life of p21 and 2KQ, the mimetic form, 2KQ exhibited consistent resistance against the degradation process (Figure 6a). As shown in Figure 2f, ubiquitin analyses of p21 and 2KQ were carried out in the absence of any specific E3 ligase. The results showed that 2KQ was almost completely resistant to the ubiquitination processes, suggesting that lysine sites 161 and 163 might be simultaneously targeted by ubiquitination (Figure 6b). The binding affinity of 2KQ for Tip60 was not significantly different from that of WT (Figure 6c). However, 2KQ levels were not affected by the presence of Tip60 (Figure 6d). The half-life of p21 protein in the presence of Tip60 was similar to that of 2KQ. On the other hand, the presence of Tip60 had no apparent effect on the 2KQ protein stability (Figure 6e). Additionally, in order to elucidate which residue between 161 and 163 on p21 is essential for ubiquitination, we performed

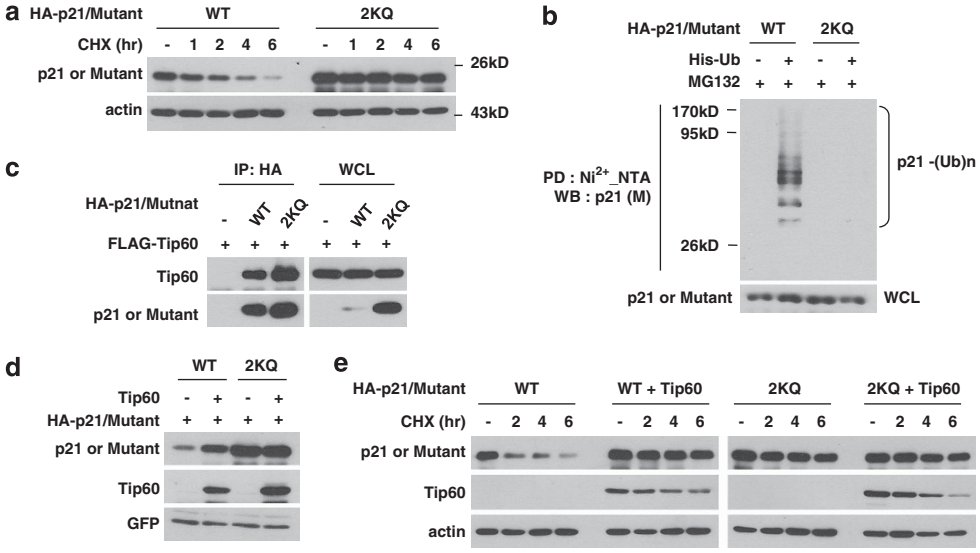

Figure 6 The acetylated p21 mimetic mutant is highly stable and protected against ubiquitination. (**a**) Prolonged stabilization of 2KQ compared with that of WT p21. Plasmids expressing HA-p21 and HA-2KQ were expressed in H1299 cells, after which CHX was added for 0, 1, 2, 4, 6 h. The resulting WCLs were then subjected to immunoblotting. (**b**) An acetylated p21 mimetic mutant is poorly targeted by general E3-ubiquitin ligases. H1299 cells were transfected with plasmids expressing HA-p21, HA-2KQ, and His-Ub. After MG132 treatment, ubiquitination assay was performed. Ubiquitinated forms of p21 were detected by anti-p21 mouse antibodies (upper panel), while expression of total levels of p21 are indicated in the bottom panel. (**c**) The binding affinity of 2KQ is similar to WT p21 toward Tip60. Plasmids expressing HA-p21, HA-2KQ and FLAG-Tip60 were transfected in 293T cells. The cell's extracts were inmmunoprecipitated with anti-HA antibodies. (**d**, **e**) p21 but not the acetylated p21 mimetic mutant 2KQ is stabilized by Tip60. H1299 cells were transfected with plasmids expressing HA-p21, HA-2KQ and Tip60 as indicated. The half-life of p21 and 2KQ were employed as described above

ubiquitin and stabilization analyses of p21, K161R, K163R, and 2KR. Both K161R and K163R mutants showed reduced levels of ubiquitination, even with more p21 expressed compared with the WT, suggesting that these sites might function additively (Supplementary Figure 15a). The role of lysines in inducing p21 ubiquitination and subsequent degradation was further analyzed by measuring the half-lives of the mutants. As expected, 2KR and 2KQ were completed protected against degradation upon treatment with CHX while K161R and K163R were partially protected from degradation (Supplementary Figures 15b). It seems that both the 161 and 163 lysine sites might contribute additively to ubiquitination labeling.

MKRN1 has been shown previously to induce p21 degradation through ubiquitination and subsequent proteasome-dependent degradation without affecting mRNA levels.[13] Introduction of MKRN1 induced the degradation of exogenous p21 protein, which was completely reversed by the addition of exogenous Tip60 (Supplementary Figure 16a). On the other hand, HAT mut did not protect p21 from MKRN1-mediated degradation (Supplementary Figure 16b). Furthermore, when MRKN1-mediated degradation of 2KQ was compared with that of the WT, only 2KQ was completely protected from degradation (Supplementary Figure 16c). Consistent with the degradation data, the presence of Tip60 almost completely diminished MKRN1-mediated ubiquitination of p21 (Supplementary Figure 16d). It seems that there was not much difference in binding affinity between MKRN1 and WT, or 2KQ (data not shown). Finally, using WT or 2KQ, ubiquitination analyses were further performed in the presence or absence of MKRN1. The data indicated that only 2KQ was extensively blocked from ubiquitination with or without MKRN1, implying that 161 and 163 sites might be simultaneously targeted by ubiquitination and as acetylation (Supplementary Figure 16e). In summary, these data show that Tip60 inhibited E3 ligase-dependent ubiquitination and degradation of p21. Furthermore, the observations that the 2KQ mutant was completely resistant to ubiquitination by MKRN1 or by other E3 ligases implied that the acetylation and ubiquitination sites of p21 might overlap.

An acetylated p21 mimetic potently induces cell-cycle arrest, growth inhibition, and senescence. To analyze the function of the acetylated form of p21, stable cell lines of $p21^{-/-}$ MEFs expressing WT p21 or 2KQ, as well as vector control, were established using a retroviral system. Population doubling analyses showed that $p21^{-/-}$ MEFs expressing 2KQ stopped proliferating after the fifth passage, while $p21^{-/-}$ MEFs with or without WT p21 were capable of proliferating past seven passages (Figure 7a). Western blot data of these cell lines showed that expression levels of 2KQ were increased compared with those of the WT (Figure 7b). These results corroborated the previous data showing that 2KQ is more stable than WT p21 (Figure 6). The significant accumulation of cyclin D1 in $p21^{-/-}$ MEFs expressing 2KQ was expected due to cell-cycle arrest at the G1 phase. Likewise, 2KQ-expressing cells were arrested at the G1 stage by a margin of 20% compared with WT p21-expressing cells (Figure 7c). Finally, SA-β-gal staining assays showed that 2KQ-overexpressing cells had a threefold increase in the number of senescent cells compared with WT p21 or p21 null cells (Figure 7d), lending further support to the data in Figure 7. Taken together, these observations suggest that the acetylated form of p21 (tested here in a mimetic form) has enhanced tumor suppressor activity due to the induction of cell-cycle arrest at the G1 phase.

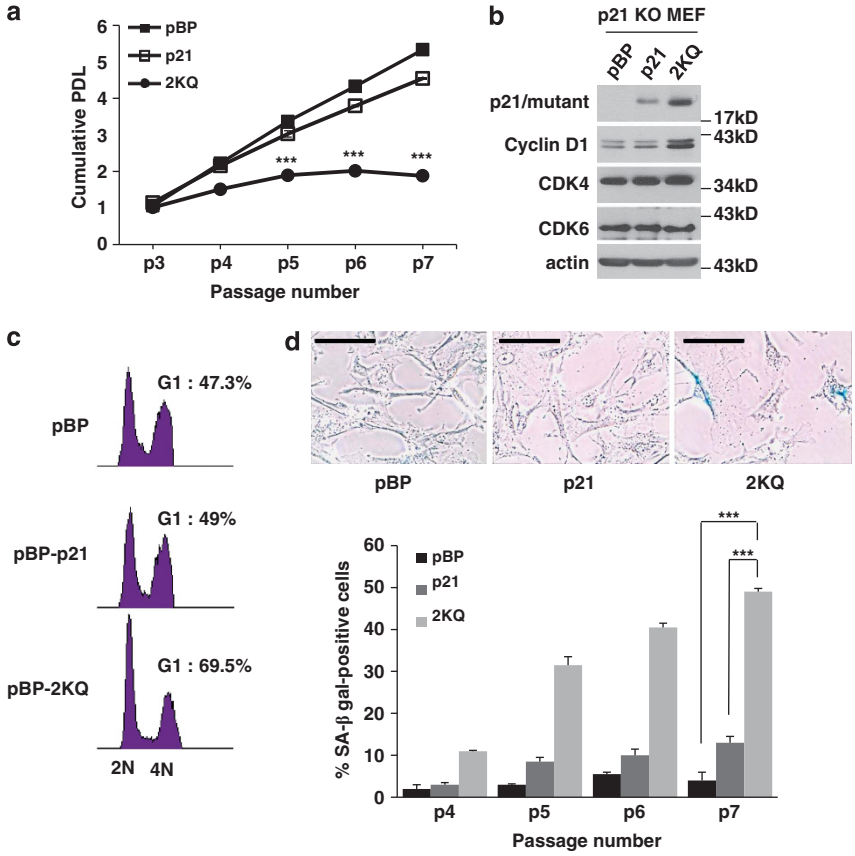

Figure 7 Acetylated p21 enhances p21-mediated cell-cycle arrest and delays the growth of p21 null MEFs. (**a**) Growth retardation of p21 null MEFs is expedited upon expression of 2KQ. p21$^{-/-}$ mouse embryonic fibroblast (MEF) cells at passage 2 were stably transduced with a retrovirus construct expressing either WT or 2KQ p21s; pBP was used as control. After puromycin selection, as described in Experimental Procedures, the growth rate of p21$^{-/-}$ MEFs stably expressing p21 or 2KQ was examined by 3T3 assay. Data are presented as the accumulated population doublings from passages 3–7. Error bars are the mean ± S.D., $n=3$ (***$P<0.001$, 2KQ compared to p21). (**b**) Increased abundance of 2KQ but not WT p21 in p21$^{-/-}$ MEF cell extracts prepared after passage 5 were analyzed by western blotting as indicated. (**c**) p21$^{-/-}$ MEFs constitutively expressing the 2KQ mutant exhibited a strong G1 phase arrest phenotype. Further, p21$^{-/-}$ MEFs (passage 7) expressing either WT p21 or 2KQ were analyzed by FACScan as described in Experimental Procedures. (**d**) p21$^{-/-}$ MEFs expressing 2KQ exhibited increased senescence compared with WT p21. The photographic images represent stained cells for SA-β-gal activity at passage 7 (upper panel, magnification: $\times$200, scale bar: 50 μm). The percentage of X-gal-stained cells examined between passages 3–7 were quantified (bottom panel). Data are the mean ± S.D. of three independent experiments. ***$P<0.001$

Discussion

The acetylation of p21 has often been suspected to be one of the main post-translational modification pathways of p21. Although this possibility has been supported by the results of previous investigations, the acetyltransferase has been unidentified, and thus the physiological importance remains unclear.

Here, we identify that Tip60 could acetylate p21 on 161 and 163 lysine sites. Tip60 acetylates p53 at lysine 120 under lethal conditions, which is an indispensable process that induces cell death by activating Bax and PUMA transcription.[22,23] As Tip60 also activates p21, Tip60 would seem to be involved in both cell death and cycle arrest processes. It has been well established that cell-cycle arrest induced by p21 upregulation could prevent or delay the apoptosis induced by p53 stimulation.[3] Tip60 activation of both pathways would seem to be contradictory with the already accepted hypothesis, which raises some questions. One interesting observation is that the interaction between Tip60 and p21 becomes weakened under lethal conditions (Supplementary Figure 12b). The acetylation of p21 is consistently attenuated, possibly destabilizing endogenous p21. The inhibition of p21 transcription under lethal conditions, and thus the prevention of the *de novo* synthesis of p21, also contributes to p21 attrition (Supplementary Figure 13).[35–37] While the reasons for the decrease in the interaction of Tip60 and p21 under lethal conditions are not clear, the possibility of unknown factors participating in these regulatory mechanisms could not be excluded.

There are other questions that still need to be addressed. For example, the induction of p21 by Tip60 or TSA could be either transcriptional or post-translational based on different cellular contexts. Levels of p21 in U2OS were affected by Tip60 depletion but not by TSA treatment. Despite the questions raised in this study, we expect that these observations of Tip60-mediated p21 acetylation might extend our knowledge of how cells could cope with environmental stresses, both moderate and lethal, through various degrees of regulatory responses.

Materials and Methods

siRNA-mediated ablation of Tip60. To ablate Tip60, three different Tip60 siRNAs were designed as described previously[22,38] and provided by Qiagen (Valencia, CA, USA): Tip60 #1 (5′-GTACGGCCGTAGTCTCAAGAA-3′), Tip60 #2 (5′-ACGGAAGGTGGAGGTGGTTAA-3′), and Tip60 #3 (5′-GGGCACCATCT CCTTCTTT-3′).

Mass spectrometry. To detect the acetylated p21 peptide and sites of acetylation, 293T cells were transfected with HA-p21-expressing plasmid alone or in combination with a Tip60-expressing plasmid and treated with 1 μM TSA (Sigma-Aldrich, St. Louis, MO, USA). WCLs were immunoprecipitated by anti-HA antibody and analyzed using SDS-PAGE. The gel was stained using a silver staining method for detection of p21. In-gel Arg-C digestion was performed as described previously.[39] The purified Arg-C digested peptides were analyzed using a LTQ-XL mass spectrometer (Thermo Finnigan, San Jose, CA, USA) coupled with an Eksigent-Nano-Ultra (Eksigent Technologies, Dublin, CA, USA). Tryptic peptides were applied to an in-house prepared analytic column (75 μm $\times$ 12 cm) packed with 5μm C18 resin. A linear 35 min gradient was achieved from 97% solvent A (0.1% formic acid in H_2O) to 60% solvent B (0.1% formic acid in ACN) at a flow rate of 300 nl/min. The separated peptide ions were electrosprayed into the nano-ESI source. The electrospray voltage was 1.8 kV, and normalized collision energy for MS/MS was 35%. All MS/MS spectra were acquired via a data-dependent scan for fragmentation of the five most abundant spectra from the full MS scan. The repeat count for dynamic exclusion was set to 1, the repeat duration was 30 s, the dynamic exclusion duration was set at 180 s, the exclusion mass width was 1.5 Da, and the list of dynamic exclusions was 50. The acquired MS/MS spectra were indexed against IPI-HUMAN.v.3.70 protein databases. Mascot (Matrix Science Inc., Boston, MA, USA, version 2.2.1) searching was performed with the following parameters: enzyme, Arg-C; fragment ion mass tolerance, 1Da; parent ion tolerance, 2Da; miss cleavage site, 2; variable modification, oxidation of Met; fixed modification, alkylation of Cys and acetylation of Lys. The resulting MS/MS spectra were validated by manual inspection of the target peptides.

Immunoprecipitation assay. Cells were lysed in a lysis buffer containing 50 mM Tris-HCl (pH 7.5), 150 mM NaCl, 0.5% Triton X-100, and 1 mM EDTA containing a protease inhibitor cocktail. The cell lysates were then incubated with 1 μg antibody for 2 h with gentle rotation followed by 30 μl protein G agarose (Peptron, Korea) for 2 h. The beads were washed three times with lysis buffer free of protease inhibitors, and the precipitated proteins were eluted in SDS sample buffer under boiling conditions. Proteins were analyzed by immunoblotting as described previously.[40]

***In vitro* and *in vivo* acetylation assays.** To detect acetylated p21 *in vitro*, protein acetylation assays were performed as previously described.[22] Briefly, HA-p21 and HA-2KR proteins were expressed in TNT Coupled Reticulocyte Lysate systems (Promega, Madison, WI, USA). Next, 2 μl of HA-p21 or HA-2KR proteins and 1 μg of purified GST-Tip60 proteins were incubated with 20 μl reaction buffer containing 50 mM Tris-HCl (pH 7.9), 10% glycerol, 1 mM DTT, 10 mM sodium butyrate, and 5 μM acetyl-CoA (A2056, Sigma-Aldrich) at 30 °C for 1 h. Acetylated proteins were detected by immunoblotting using α-Acetyl K antibodies or α-AcK161/163-p21 antibodies.

To detect ectopically expressed or endogenous acetylated p21, cells were lysed in lysis buffer containing 5 μM TSA and 0.3% SDS. The cell lysates were combined with 5 μl of α-Acetyl K antibodies or 10 μl of α-AcK161/163-p21 antibodies and then incubated overnight with gentle rotation. Afterwards, 30 μl of protein G agarose beads were added and incubated for an additional 2 h. Beads were washed three times using lysis buffer, and the precipitated proteins were eluted in SDS sample buffer under boiling conditions. The acetylated p21 was detected by immunoblotting using anti-p21 antibodies.

Reverse transcription (RT)-PCR analysis. Using Trizol reagent (Invitrogen, Carlsbad, CA, USA), total RNA was prepared, and cDNA was amplified using 1 μg of total RNA as previously described.[13] cDNA was analyzed using QuantiTect SYBR Green PCR Kit and real-time PCR (Rotor-Gene Q 2plex, Qiagen). Cycling conditions: 95 °C for 10 min, 40 cycles at 95 °C for 5 s and 95 °C for 45 s. The primer sequences used were: human p21, 5′-G ACTCTCAGGGTCGAAAACG-3′ (forward) and 5′-GGCGTTTGGAGTGGTA GAAA-3′ (reverse); human Tip60, 5′-ATGGCGGAGGTGGGGGAGATA-3′ (forward) and 5′-TTAGCGTGGTGCTGACGGTAT-3′ (reverse); human glyceraldehyde-3-phosphate dehydrogenase (GAPDH), 5′-GATCATCAGCAA TGCCTCCT-3′ (forward) and 5′-TGTGGTCATGAGTCCTTCCA-3′.

Plasmid and reagents. Rabbit anti-p21 (C-19), goat anti-Tip60 goat (N-17), mouse HA (F-7), rabbit HA (Y-11), mouse ubiquitin (P4D1), mouse GST (B-14), rabbit GFP (FL), mouse Myc (9E10), normal mouse IgG, and normal rabbit IgG antibodies were purchased from Santa Cruz Biotechnology (Santa Cruz, CA, USA). Mouse anti-FLAG (M2), rabbit FLAG (F7425), and mouse β-actin (A5316) antibodies were purchased from Sigma-Aldrich. Mouse anti-p21 (#2946) and rabbit acetylated-lysine (#9441) antibodies were purchased from Cell Signaling Technology (Danvers, MA, USA). The rabbit anti-Tip60 antibody was kindly provided by Bruno Amati (European Institute of Oncology [IEO], Italy). Propidium iodide (P4170), CHX (C4859), trypan blue (T8154), SAHA, sodium butyrate and dimethyl sulfoxide were purchased from Sigma-Aldrich. MG132 was purchased from Calbiochem (San Diego, CA, USA), and adriamycin was purchased from Duchefa (Haarlem, The Netherlands). HA-p21 and FLAG-p21 were constructed in pcDNA3 as described previously.[13] Deletion mutants of p21, the KR mutants and the 2KQ mutant were generated by polymerase chain reaction (PCR) and constructed into pCS3-MT-BX, pcDNA3-HA and pcDNA3-FLAG. p21, 2KR, and 2KQ cDNA were also subcloned into pBABE-puro. p3XFLAG-CMV-Tip60 and p3XFLAG-CMV-HATmut were kindly provided by SH Baek (Seoul National University, Korea). ΔHAT cDNA was prepared by PCR and subcloned into p3XFLAG-CMV. Deletion mutants of Tip60 were also generated by PCR and constructed into p3XFLAG-CMV. pcDNA3.1-MKRN1, and pcDNA3-FLAG-MKRN1,[13] pcDNA3-His-Ub[41] were described previously. pEGFP-C2 vector (Clontech, San Diego, CA, USA) was used as a transfection control.

Protein purification and GST pulldown. p21 cDNA was prepared using restriction enzymes (*Eco*RI and *Xho*I) and subcloned into the pET28a plasmid vector (Novagen, San Diego, CA, USA) that contained a hexa-histidine tag at the C-terminus. p21 protein was purified from *Escherichia coli* using Ni-NTA affinity chromatography (Qiagen) and size exclusion chromatography (Superdex 200; GE Healthcare, Buckinghamshire, UK). GST-Tip60 protein was purified from bacteria using GST Sepharose beads according to the manufacturer's protocol (GE Healthcare). As indicated, His-p21 was incubated with GST or GST-Tip60 for 2 h, followed by addition of GST Sepharose beads and 2 h of incubation. Finally, the beads were washed and eluted in 10 mM reduced glutathione.

Ubiquitination assay. To validate the ubiquitinated forms of p21, the ubiquitination assay was conducted under the denaturation condition as described previously.[13] Briefly, cells were lysed in 6 M guanidium-HCl buffer (pH 8) containing 5 mM *N*-ethylmaleimide (NEM; Sigma-Aldrich) to interfere with deubiquitination. Using Ni^{2+}-NTA beads (Qiagen), His-ubiquitin-conjugated proteins were pulled-down and washed.

To detect endogenous p21 ubiquitination under denaturation, cells were lysed in PBS containing 1% SDS and 5 mM NEM and then boiled for 10 min. WCLs were immunoprecipitated with anti-p21 antibodies in lysis buffer (a final concentration of 0.1% SDS). For immunoblotting, proteins were transferred to PVDF membranes and denatured using 6 M guanidine-HCl containing 20 mM Tris-HCl (pH 7.5), 5 mM mercaptoethanol, and 1 mM PMSF for 30 min at 4 °C. Ubiquitinated p21 was identified by HRP-conjugated anti-Ub antibodies (FK2, PW0150, biomol).

Retroviral transduction. To develop stable p21- and 2KQ-expressing cell lines, the respective cDNAs were subcloned into a pBABE-puro plasmid, which has a puromycin resistance gene. 293T cells were transfected with pBABE (control), pBABE-p21, or pBABE-2KQ together with VSV-G and a gag-pol-expressing vector followed by incubation for 48 h in order to produce packaged retroviruses. p21 null MEF cells were infected with the packaged retroviruses expressing p21 or its mutants. Finally, to select for retrovirus infected cells, cell lines were incubated in 2 μg/ml Puromycin (Sigma-Aldrich).

Cell culture and transfection. HCT116 $p53^{+/+}$, HCT116 $p53^{-/-}$ (kindly provided by Dr. B Vogelstein, Johns Hopkins University, Baltimore, MD, USA), H1299, HeLa, 239T cell lines, and p21 null MEF[42] were maintained in Dulbecco's Modified Eagle's Medium supplemented with 10% fetal bovine serum (FBS) and 1% penicillin/streptomycin (Thermo Scientific, Franklin, MA, USA). All cell lines were incubated in 5% CO_2 at 37 °C. Plasmid DNA was transfected using Lipofectamine 2000 (Invitrogen), and the siRNA was transfected using Lipofectamine RNAiMAX according to the manufacturer's protocol.

FACS analysis. To analyze cells in a given cell-cycle phase, cells were fixed in 70% ethanol and incubated with 100 mg/ml of RNase A (Qiagen) for 30 min, followed by 10 mg/ml of propidium iodide (Sigma-Aldrich) for 30 min. Cell-cycle analysis was performed using a FACScan apparatus (BD Biosciences, Franklin Lakes, NJ, USA).

SA-β-galactosidase assay. For staining of senescent cells, a senescence detection kit (#K320-250, BioVision, Mountain View, CA, USA) was used. Briefly, plated cells were washed with PBS and then fixed with fixation solution for 15 min at RT. Cells were washed two times with PBS and then incubated with staining solution overnight at 37 °C. The stained cells were observed and manually counted using a microscope.

Statistical data analysis. To validate the significance of differences between groups, one-way ANOVA and the unpaired two-tailed *t*-test were applied via Prism (version 5.0; GraphPad, La Jolla, CA, USA).

Conflict of Interest

The authors declare no conflict of interest.

Acknowledgements. This work was supported by the National Research Foundation of Korea (NRF) grant funded by the Korean government (MEST) (2010-0017787), a grant of the Korean Health Technology R&D Project, Ministry of Health & Welfare, Republic of Korea (A110961) and WCU (World Class University) program (Project No. R33-10128) through the National Research Foundation of Korea (NRF) funded by the Ministry of Education, Science, and Technology.

1. Harper JW, Adami GR, Wei N, Keyomarsi K, Elledge SJ. The p21 Cdk-interacting protein Cip1 is a potent inhibitor of G1 cyclin-dependent kinases. *Cell* 1993; **75**: 805–816.
2. Cazzalini O, Scovassi AI, Savio M, Stivala LA, Prosperi E. Multiple roles of the cell cycle inhibitor p21(CDKN1A) in the DNA damage response. *Mutat Res* 2010; **704**: 12–20.
3. Abbas T, Dutta A. p21 in cancer: intricate networks and multiple activities. *Nat Rev Cancer* 2009; **9**: 400–414.
4. Jung YS, Qian Y, Chen X. Examination of the expanding pathways for the regulation of p21 expression and activity. *Cell Signal* 2010; **22**: 1003–1012.
5. el-Deiry WS, Harper JW, O'Connor PM, Velculescu VE, Canman CE, Jackman J *et al.* WAF1/CIP1 is induced in p53-mediated G1 arrest and apoptosis. *Cancer Res* 1994; **54**: 1169–1174.
6. el-Deiry WS, Tokino T, Velculescu VE, Levy DB, Parsons R, Trent JM *et al.* WAF1, a potential mediator of p53 tumor suppression. *Cell* 1993; **75**: 817–825.
7. Touitou R, Richardson J, Bose S, Nakanishi M, Rivett J, Allday MJ. A degradation signal located in the C-terminus of p21WAF1/CIP1 is a binding site for the C8 alpha-subunit of the 20S proteasome. *EMBO J* 2001; **20**: 2367–2375.
8. Wang JA, Fan S, Yuan RQ, Ma YX, Meng Q, Goldberg ID *et al.* Ultraviolet radiation down-regulates expression of the cell-cycle inhibitor p21WAF1/CIP1 in human cancer cells independently of p53. *Int J Radiat Biol* 1999; **75**: 301–316.
9. Lu Z, Hunter T. Ubiquitylation and proteasomal degradation of the p21(Cip1), p27(Kip1) and p57(Kip2) CDK inhibitors. *Cell Cycle* 2010; **9**: 2342–2352.
10. Sheaff RJ, Singer JD, Swanger J, Smitherman M, Roberts JM, Clurman BE. Proteasomal turnover of p21Cip1 does not require p21Cip1 ubiquitination. *Mol Cell* 2000; **5**: 403–410.
11. Ng CC, Arakawa H, Fukuda S, Kondoh H, Nakamura Y. p53RFP, a p53-inducible RING-finger protein, regulates the stability of p21WAF1. *Oncogene* 2003; **22**: 4449–4458.
12. Starostina NG, Kipreos ET. Multiple degradation pathways regulate versatile CIP/KIP CDK inhibitors. *Tr Cell Biol* 2012; **22**: 33–41.
13. Lee EW, Lee MS, Camus S, Ghim J, Yang MR, Oh W *et al.* Differential regulation of p53 and p21 by MKRN1 E3 ligase controls cell cycle arrest and apoptosis. *EMBO J* 2009; **28**: 2100–2113.
14. Zhi X, Zhao D, Wang Z, Zhou Z, Wang C, Chen W *et al.* E3 ubiquitin ligase RNF126 promotes cancer cell proliferation by targeting the tumor suppressor p21 for ubiquitin-mediated degradation. *Cancer Res* 2012 (In press).
15. Li Z, Zhang Q, Mao JH, Weise A, Mrasek K, Fan X *et al.* An HDAC1-binding domain within FATS bridges p21 turnover to radiation-induced tumorigenesis. *Oncogene* 2010; **29**: 2659–2671.
16. Kamine J, Elangovan B, Subramanian T, Coleman D, Chinnadurai G. Identification of a cellular protein that specifically interacts with the essential cysteine region of the HIV-1 Tat transactivator. *Virology* 1996; **216**: 357–366.
17. Utley RT, Cote J. The MYST family of histone acetyltransferases. *Curr Top Microbiol Immunol* 2003; **274**: 203–236.
18. Ikura T, Tashiro S, Kakino A, Shima H, Jacob N, Amunugama R *et al.* DNA damage-dependent acetylation and ubiquitination of H2AX enhances chromatin dynamics. *Mol Cell Biol* 2007; **27**: 7028–7040.
19. Jha S, Shibata E, Dutta A. Human Rvb1/Tip49 is required for the histone acetyltransferase activity of Tip60/NuA4 and for the downregulation of phosphorylation on H2AX after DNA damage. *Mol Cell Biol* 2008; **28**: 2690–2700.
20. Avvakumov N, Cote J. The MYST family of histone acetyltransferases and their intimate links to cancer. *Oncogene* 2007; **26**: 5395–5407.
21. Squatrito M, Gorrini C, Amati B. Tip60 in DNA damage response and growth control: many tricks in one HAT. *Tr Cell Biol* 2006; **16**: 433–442.
22. Tang Y, Luo J, Zhang W, Gu W. Tip60-dependent acetylation of p53 modulates the decision between cell-cycle arrest and apoptosis. *Mol Cell* 2006; **24**: 827–839.
23. Sykes SM, Mellert HS, Holbert MA, Li K, Marmorstein R, Lane WS *et al.* Acetylation of the p53 DNA-binding domain regulates apoptosis induction. *Mol Cell* 2006; **24**: 841–851.
24. Charvet C, Wissler M, Brauns-Schubert P, Wang SJ, Tang Y, Sigloch FC *et al.* Phosphorylation of Tip60 by GSK-3 determines the induction of PUMA and apoptosis by p53. *Mol Cell* 2011; **42**: 584–596.
25. Jiang Z, Kamath R, Jin S, Balasubramani M, Pandita TK, Rajasekaran B. Tip60-mediated acetylation activates transcription independent apoptotic activity of Abl. *Mol Cancer* 2011; **10**: 88.
26. Lin SY, Li TY, Liu Q, Zhang C, Li X, Chen Y *et al.* GSK3-TIP60-ULK1 signaling pathway links growth factor deprivation to autophagy. *Science* 2012; **336**: 477–481.
27. Lee EJ, Shin SH, Hyun S, Chun J, Kang SS. Endoplasmic reticulum (ER) stress enhances Tip60 (A histone acetyltransferase) binding to the Concanavalin A. *Open Biochem J 2012; 6: 1–10.*
28. Cheng Z, Ke Y, Ding X, Wang F, Wang H, Wang W *et al.* Functional characterization of TIP60 sumoylation in UV-irradiated DNA damage response. *Oncogene* 2008; **27**: 931–941.
29. Gorrini C, Squatrito M, Luise C, Syed N, Perna D, Wark L *et al.* Tip60 is a haplo-insufficient tumour suppressor required for an oncogene-induced DNA damage response. *Nature* 2007; **448**: 1063–1067.
30. Gevry N, Chan HM, Laflamme L, Livingston DM, Gaudreau L. p21 transcription is regulated by differential localization of histone H2A.Z. *Genes Dev* 2007; **21**: 1869–1881.
31. Park JH, Sun XJ, Roeder RG. The SANT domain of p400 ATPase represses acetyltransferase activity and coactivator function of TIP60 in basal p21 gene expression. *Mol Cell Biol* 2010; **30**: 2750–2761.
32. Gui CY, Ngo L, Xu WS, Richon VM, Marks PA. Histone deacetylase (HDAC) inhibitor activation of p21WAF1 involves changes in promoter-associated proteins, including HDAC1. *Proc Natl Acad Sci USA* 2004; **101**: 1241–1246.
33. Ikura T, Ogryzko VV, Grigoriev M, Groisman R, Wang J, Horikoshi M *et al.* Involvement of the TIP60 histone acetylase complex in DNA repair and apoptosis. *Cell* 2000; **102**: 463–473.
34. Abbas T, Sivaprasad U, Terai K, Amador V, Pagano M, Dutta A. PCNA-dependent regulation of p21 ubiquitylation and degradation via the CRL4Cdt2 ubiquitin ligase complex. *Genes Dev* 2008; **22**: 2496–2506.
35. Kim JH, Chae M, Kim WK, Kim YJ, Kang HS, Kim HS *et al.* Salinomycin sensitizes cancer cells to the effects of doxorubicin and etoposide treatment by increasing DNA damage and reducing p21 protein. *Br J Pharmacol* 2011; **162**: 773–784.
36. Tsuchiya N, Izumiya M, Ogata-Kawata H, Okamoto K, Fujiwara Y, Nakai M *et al.* Tumor suppressor miR-22 determines p53-dependent cellular fate through post-transcriptional regulation of p21. *Cancer Res* 2011; **71**: 4628–4639.
37. Seoane J, Le HV, Massague J. Myc suppression of the p21(Cip1) Cdk inhibitor influences the outcome of the p53 response to DNA damage. *Nature* 2002; **419**: 729–734.
38. Kim JH, Kim B, Cai L, Choi HJ, Ohgi KA, Tran C *et al.* Transcriptional regulation of a metastasis suppressor gene by Tip60 and beta-catenin complexes. *Nature* 2005; **434**: 921–926.
39. Hubner NC, Ren S, Mann M. Peptide separation with immobilized pI strips is an attractive alternative to in-gel protein digestion for proteome analysis. *Proteomics* 2008; **8**: 4862–4872.
40. Oh W, Lee EW, Sung YH, Yang MR, Ghim J, Lee HW *et al.* Jab1 induces the cytoplasmic localization and degradation of p53 in coordination with Hdm2. *J Biol Chem* 2006; **281**: 17457–17465.
41. Camus S, Higgins M, Lane DP, Lain S. Differences in the ubiquitination of p53 by Mdm2 and the HPV protein E6. *FEBS Lett* 2003; **536**: 220–224.
42. Sung YH, Kim HJ, Devkota S, Roh J, Lee J, Rhee K *et al.* Pierce1, a novel p53 target gene contributing to the ultraviolet-induced DNA damage response. *Cancer Res* 2010; **70**: 10454–10463.

Supplementary Information accompanies the paper on Cell Death and Differentiation website (http://www.nature.com/cdd)